Texture and Morphology of Biaxially Stretched Poly(ethylene naphthalene-2,6-dicarboxylate)

A. Douillard,[1] L. Hardy,[1] I. Stevenson,[1] G. Boiteux,[1] G. Seytre,[1] T. Kazmierczak,[2] A. Galeski[2]

[1]*Laboratoire des Matériaux Polymères et des Biomatériaux, UMR CNRS 5627, Université Claude Bernard—Lyon 1, Bat.ISTIL, 43 Blvd du 11 novembre 1918, 69622 Villeurbanne cedex, France*
[2]*Centre of Molecular and Macromolecular Studies, Polish Academy of Sciences, 90-363 Lodz, Sienkiewicza 112, Poland*

Received 17 September 2002; accepted 13 November 2002

ABSTRACT: The orientation of poly(ethylene naphthalene-2,6-dicarboxylate) (PEN) films with different morphologies were studied by wide-angle X-ray diffraction. Different structures were obtained by thermally treating biaxially stretched PEN samples. Virgin and thermally treated (1 h at 240, 250, and 260°C) samples of PEN bioriented films were characterized by DSC to determine the glass-transition temperature and the crystallinity ratio. To define the orientation of crystallites in the 25 μm thick bioriented samples, pole figures were recorded for various PEN samples, as a function of their position in the transverse drawing direction. The significant result is that there is a dominant crystal population, whose *c*-axis direction varies from +45° at one sample edge to −45° at the other edge, the orientation at the center being parallel to the transverse direction. There is also a secondary population, which can be seen only near the center. DSC studies also showed that by increasing the annealing temperature the crystallinity ratio was increased and pole figures showed that the texture was modified, probably because of disorientation mainly from an annealing temperature of 260°C. © 2003 Wiley Periodicals, Inc. J Appl Polym Sci 89: 2224–2232, 2003

Key words: morphology; pole figure; texture; orientation; poly(ethylene naphthalene-2,6-dicarboxylate) (PEN)

INTRODUCTION

Poly(ethylene naphthalene-2,6-dicarboxylate) (PEN) is a thermoplastic polyester possessing a combination of good thermal stability, degradation resistance, good mechanical and dielectric properties, low dielectric loss factor, and low permeability.[1] The physical properties of PEN are similar or superior to those of polyethylene terephthalate (PET) and can be obtained as very thin (1 μm) films at reasonable cost. Like PET films, PEN films are used as dielectric material in capacitors but can also compete with PET in the packaging industry or as a substrate in magnetic media (audio, video, or computer data storage).[2,3] Because PEN is mainly used in the form of thin films, which can be obtained by uniaxial or biaxial stretching, the understanding of the evolution of its morphology and orientation with temperature and stretching conditions is essential to adjust its properties for a given application. During the last two decades, relatively few studies have been found in the literature about such a polymer. Those published deal mainly with structure, orientation, and dielectric and photoconduction properties.[4–11]

The general formula of PEN is $(–CH_2–O–CO–C_{10}H_6–CO–O–CH_2–)_n$, whose centro-symmetric backbone is shown on Figure 1. From this figure, it may be seen that the chain structure of PEN is similar to that of PET but the naphthalene group of PEN as opposed to the phenyl group in PET leads to a stronger rigidity of the macromolecular chain and thus a superior thermal and mechanical resistance than PET. PEN can crystallize under two triclinic forms[4]: α and β, which have been characterized[5] by WAXS. The α-form corresponds to one chain per unit cell and this so-called low temperature form crystallizes from the melt at 160°C after melting at 280°C. The β-form has two chains per unit cell in which the naphthalene group undergoes a 180° rotation around the bond axis linking the carbon atoms in the 4 and 4′ positions. The so-called high-temperature β-form can be obtained by melting the sample above 330°C, followed by a crystallization at 245°C reached after a rapid cooling. It is also possible to crystallize the sample in this form by quenching it from the melt to room temperature and then rapidly heating it to 245°C. Generally, the α-form is obtained because the β-form is more difficult to nucleate. If the α-form has been formed once, it will appear again even if the sample has been melted at 300°C and crystallized again.

Correspondence to: I. Stevenson (isabelle.stevenson@univ-lyon1.fr).

Contract grant sponsor: Ministry of Education and Research.

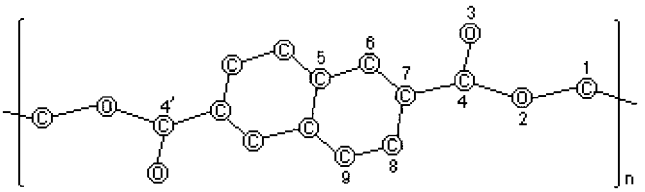

Figure 1 PEN backbone formula.

Studies by Cakmak et al.[6] have shown a necking formation phenomenon during the polymer drawing between the glass-transition temperature (T_g) and the cold crystallization temperature. Necking formation at a temperature lower than or near to T_g is also observed for PET. For oriented samples, although crystallinity increases, the refractive index in the direction normal to the PEN film decreases when the uniaxial drawing ratio increases, which has already been observed for PET. This behavior is linked to the preferential orientation of the phenyl ring parallel to the surface; thus the naphthalene rings of PEN will be aligned parallel to the film surface during drawing. An increase of crystallinity is observed in biaxially stretched annealed PEN films. Such films crystallize in the α-form and as the crystallite orientation increases, the quantity of the β-form decreases.[7]

Studies of orientation of the chains in the machine direction (MD) and the transverse direction (TD) were previously reported.[6,8] The elastic modulus of a semicrystalline polymer gives important information on the molecular conformation and the intermolecular forces in the crystalline network. Nakamae et al.[9,10] measured the elastic modulus on biaxially stretched PEN and analyzed the deformation by X-ray diffraction in a parallel direction to the main axis of the polymer. These measurements allow the elastic modulus E to be related to the crystalline network deformation. These authors showed that the strength necessary to stretch the sample by 1% was higher for PEN than for PET because of the naphthalene ring rigidity and its fully extended structure. PET is well known to contract from its fully extended conformation by an internal rotation around the O–CH_2 bonds. In contrast, all the atoms in the PEN chain, O–CH_2 included, are coplanar. Typical differences in the mechanical properties of biaxially stretched PEN and PET films are reported elsewhere.[4,6]

The elastic modulus, the tensile strength, and the elongation at break of PEN in the machine direction and the transverse direction will depend on the process conditions. The shrinkage values are lower than those of PET for an equivalent orientation. Rueda et al.[11] related microhardness to the structure of PEN. The increase of hardness can be explained only by an increase in crystallinity and the development of the thickness of the crystals must be taken into account. When studying the biaxial drawing of oriented polymers, Jungnickel et al.[12,13] produced equations relating the degree of orientation caused by biaxial nonorthogonal pseudoaffine deformation to the conditions and parameters of the deformation, which have been derived.[12] These equations have been used to correlate the degree of orientation of PET with drawing parameters.[13] The bowing of the film has been analyzed in terms of viscous and elastic components of the deformation and of lateral stress distribution across the film.

EXPERIMENTAL

Bistretched PEN 25 μm thick samples were obtained from Du Pont de Nemours as 2300 mm wide films in the transverse direction (TD), which is the full production width. The molecular weight of the polymer could not be obtained. Bioriented PEN films were obtained by a sequential bistretching in two directions (at 90° to each other) with a first stretching in the machine direction (MD) at 145°C then in the TD direction at the same temperature from the 300 μm thick amorphous film studied in a previous investigation.[14] The draw ratio λ for MD and TD was constituted between 3.5 and 4 and the ratio TD/MD = 1. PEN films are annealed at 250°C in the industrial process (also called thermosetting temperature and chosen 10 to 30 K below melting temperature), which is used to make the film more stable for heat shrinkage. From this film, 16 samples were indexed, as shown in Figure 2. (The meaning for the indexation letters used can be found in this figure caption.) The thermal treatments consisting in annealing at temperatures equal to 240, 250, and 260°C, respectively, were applied to the aF and dF parts of these films. Samples were treated in the oven of a dynamic mechanical instrument described elsewhere[14] for 1 h and then slowly cooled to room temperature (controlled cooling rate of 5 K/min) before analysis. The effect of such thermal treatments leads to a modification of the initially oriented morphology of the samples. The annealing was carried out totally free, so samples were under no restraint that would prevent shrinkage in both directions.

To obtain pole figures, a WAXS system was used that consisted of a computer-controlled pole figure device associated with a wide-angle goniometer coupled to an X-ray tube operating at 30 kV and 30 mA (Cu–K_α radiation, filtered electronically and by Ni filter). The complete pole figures were obtained for the stereographic projection of Euler angles of crystal orientation with respect to the incident beam φ (polar angle) in the range from 0 to 90° and ψ (azimuthal angle) from 0 to 360°, both in 5° steps (see Fig. 3). The complete pole figures were then obtained for φ = 0–50° by reflection and φ = 50–90° by transmission; the connecting angle was φ_c = 50°. The slit system was

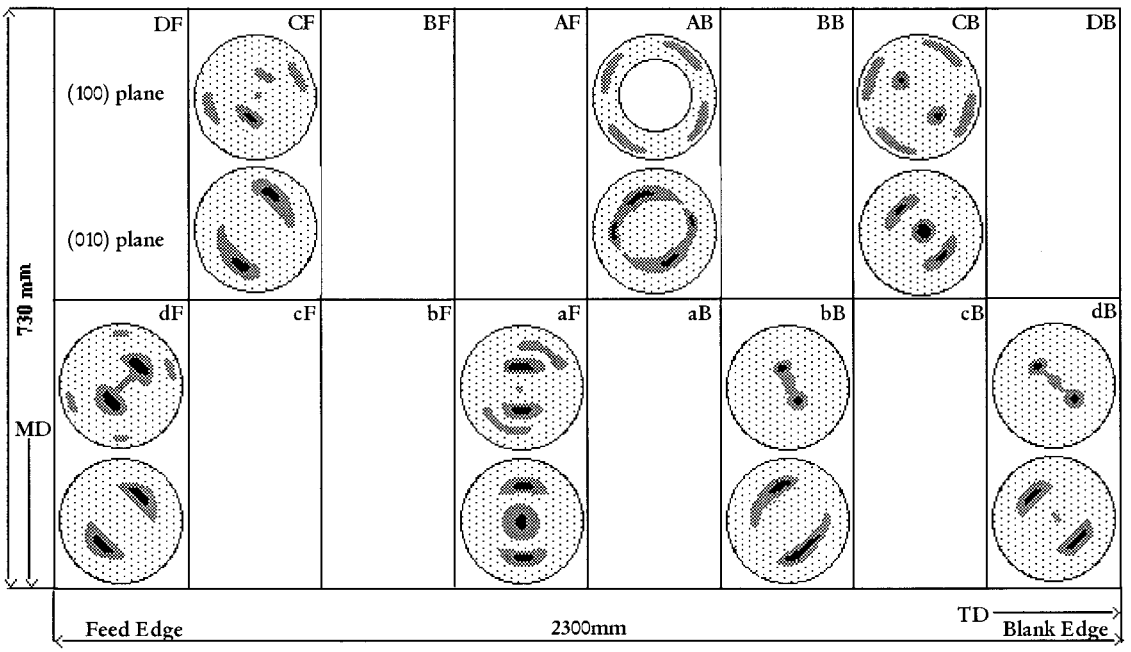

Figure 2 (1 0 0) and (0 1 0) pole figures and indexation of the different parts of the PEN samples studied within the width of the film. F, feed edge; B, blank edge. Four positions named a, b, c, d or A, B, C, D were chosen from the center of the film: lowercase letters correspond to the bottom part of the film and capital letters to the top of the film.

always adjusted to measure the integral intensity of the appropriate diffraction peak. The necessary corrections for background scattering and sample absorption were calculated. The diffraction data were then corrected for the X-ray defocusing and other instrumental effects from the data obtained in the same experimental conditions for a nonoriented PEN standard sample.

Finally, the stereographic projections were generated from the program POD, part of the pop LA package (Los Alamos National Laboratory, NM). All pole figures were plotted with linear intensity scale. The pole densities were first self-normalized to the random pole distribution and finally plotted in the units of multiplication of the density of random distribution.

DSC measurements were carried out by use of a 2920 TA Instruments apparatus in the range of 50 to 300°C with a heating rate of 10 K/min. Glass-transition temperatures were measured at the onset and

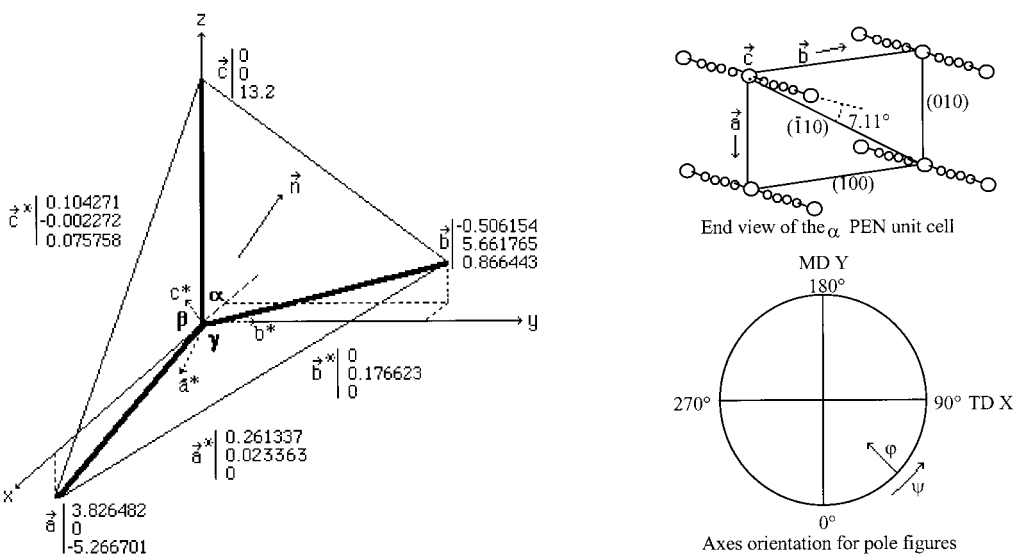

Figure 3 Coordinates of the direct and reciprocal axes of the α-form PEN in the orthonormal reference. End view of the α-PEN unit cell. Axes orientation for pole figures.

TABLE I
Coordinates of Some Atoms of the Naphthalene Ring in the Triclinic Axes[a]

Atom	Axis		
	x	*y*	*z*
C6	0.848	0.793	0.056
C8	0.122	0.171	0.207
C9	0.190	0.266	0.131

[a] See Figure 1.

midpoints. Sample weights were approximately 10 mg. Temperature calibration was obtained using indium. All samples were sealed in aluminum pans and measurements were performed under a high-purity nitrogen atmosphere.

TMA measurements were performed on a 2980 TA Instruments apparatus (also used for all thermal treatments, described in a previous study[14]). Thermal deformations were studied for aF, dB, and dF samples both in the MD and TD in the range of 50 to 300°C with a heating rate of 3 K/min.

Crystallographic properties of PEN will be detailed before studying the orientation of crystallites in the PEN films

Crystallographic data of PEN

Crystallographic data[4] for the triclinic P_{-1} unit cell of the α-phase of PEN are as follows: a = 6.51 Å, b = 5.75 Å, c = 13.2 Å, α = 81°20′, β = 144°, γ = 100°, V = 285.57 Å^3, d = 1.407 g/cm^3.

The normalized coordinates of the normal to the (hkl) planes and also the normal to the naphthalene ring were calculated for the α-phase from the triclinic parameters and from the coordinates of three atoms of the naphthalene ring (see Table I), using results obtained by Mencik et al..[4] The following orthonormal reference were used: Oz in the *c* direction, Ox orthogonal to Oz in the (a,c) plane, and Oy orthogonal to the (a,c) plane. The normal n_{hkl} to the (hkl) plane was easily calculated from the coordinates of a*, b*, and c* of the reciprocal cell as shown on Figure 3 and according to

$$\vec{n}_{hkl} = \frac{h\vec{a}^* + k\vec{b}^* + l\vec{c}^*}{\sqrt{h^2a^{*2} + k^2b^{*2} + l^2c^{*2}}} \quad (1)$$

The, (100), (010) (−110), and (−210) reticular planes of the α-phase, which have the highest diffracted intensities, were studied according to the topography of the 25 μm thick PEN film, that is, the position of the sample with respect to the transverse direction of drawing (results are reported in Table II).

The respective dihedral angles between the planes and between their normal to the planes (modulo 180°) can then be calculated (from the vectorial product for instance):

(100), (010) = 95.11° (84.89°) (the intersection of these two planes defines the *c*-axis direction)
(100), (−110) = 35.50° (144.5°) [(−110) containing the chains]
(100), (−210) = 19.06° (160.93°)
(010), (−110) = 59.61° (120.4°)
(010), (−210) = 76.04° (103.96°)
(100), (plane of the chain) = 28.39°
(010), (plane of the chain) = 66.72°
(−110), (plane of the chain) = 7.11°

Thus the angle between the normal to the chain and the normal to the (−110) plane is 7.11°; that is, the (−110) plane containing the chains has the highest electronic density (i.e., structure factor F[4] as can be seen in Table II).

The morphology and texture of bistretched PEN films can then be analyzed to relate them to mechanical and electrical properties.

RESULTS AND DISCUSSION

Determination of crystal orientation

The general view of (100) and (010) reticular plane pole figures clearly shows that the orientation of crystals (partially for aF, AB, and also CB, which behave as a second orientation group) is mainly uniaxial in the film plane and position dependent with respect to TD.

TABLE II
Reticular Planes and Coordinates of Their Normalized Normals in the Orthonormal Axes

hkl	*x* (*n*)	*y* (*n*)	*z* (*n*)	d_{hkl} (Å)	2θ[°(Cu–K$_\alpha$)]	[*F*] measured[a]	[*F*] calculated[a]
(100)[b]	0.9960	0.0890	0	3.8113	23.339	66	62
(010)[b]	0	1	0	5.6618	15.651	47	46
(001)	0.8088	−0.0176	0.5876	7.7576	11.406	17	19
(−110)[b]	−0.8626	0.5058	0	3.3008	27.012	81	84
(−210)[b]	−0.9704	0.2411	0	1.8501	49.189	52	49
Planar chain	−0.9187	0.3950	0.0065	—	—	—	—

[a] From Mencik.[4]
[b] Reticular planes used for pole figures.

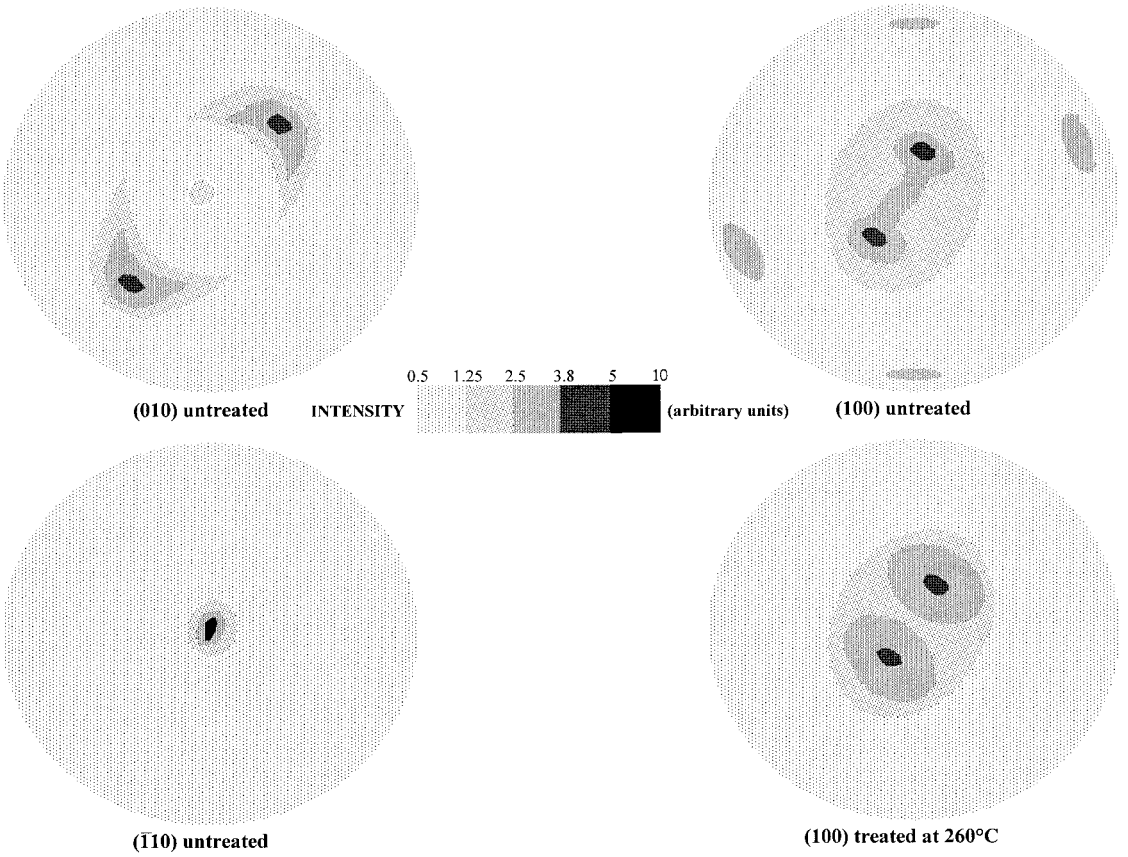

Figure 4 dF sample pole figures: (0 1 0), (1 0 0), (−1 1 0) untreated, and (1 0 0) treated at 260°C.

Because the (−110) reticular plane of the dF sample containing the chains is parallel to the film plane, the *c*-axis of the crystals must be situated within it. Figure 2 shows the pole figures (010) and (100) for the whole nontreated film and Figure 4 shows the pole figures only for the dF sample but untreated and treated at 260°C.

More precisely, the values for respective latitudes φ_1, φ_2 (in the range 0–90°) and meridians ψ_1, ψ_2 (in the range 0–180°) of two reticular planes measured according to their position in the film are summarized in Table III, which also gives the "Angle 1–2" as a verification of the good agreement for the angles of the two planes [84.9° ≅ 85° for (100) and (010)], ψ_1 and ψ_2 being adjusted modulo 180°, that is, taken in the range 0–360° for this purpose. The coordinates x_{1-2}, y_{1-2}, and z_{1-2} of the normalized vector orthogonal to the two (hkl) vectors (i.e., the direction of the intersection of the two reticular planes) are also reported. Finally, the orientations (latitude and meridian) of the *c*-axis and the dihedral angle of the chain related to the plane of the film according to the position of the sample are shown in Table IV. This table shows the separation between the main population (number 1 added to the letters indicating the positions in the processed film), the effect of annealing and the secondary population (numbers 2 and 3, respectively). It is clear that the reticular planes (100) and (010) define without doubt the orientation of the *c*-axis of the crystals in the film. For all samples, the plane of the chain is in the plane of the film within ±5°. It can be found that the plane of the chains is also in the plane of the film when looking at the orientation of the secondary population of crystals in samples aF and CB, although these populations are in higher quantity in this case.

Samples dF, CF, aF, AB, and CB, which also show other types of orientation but to a lesser extent, are described in Table III. This second family of crystals is quite as important for aF and CB samples; they exhibit a random orientation for the (100) pole with the (010) pole perpendicular to the film plane. For the particular value (aF2 in Table III), the dihedral angle between the planar chain and the film plane is 79°, approaching the perpendicular direction to the film. As for the CB sample, similarly to the aF sample, the two CB2 and CB3 in Table III are more precisely defined. Also, the plane of the chain is not situated in the film plane (its dihedral angle being 79°), but the *c*-axis is.

Concerning the (−210) reticular plane (structure factor 52), because it is in the vicinity of the (0−31) and (−316) planes of structure factors 25 and 14, respectively, at $d \cong 1.84$ Å, the pole figures are more com-

TABLE III
Calculations of Angles from Pole Figures[a]

Sample	Planes 1 and 2	φ_1 (<90°)	ψ_1 (°)	φ_2 (<90°)	ψ_2 (°)	Angle 1–2	x_{1-2}	y_{1-2}	z_{1-2}
dF annealed	(100) (010)	57	135	28	316*	85	0.6978	0.7169	−0.0084
dF annealed	(100) (−110)	57	135	90	any	33	0.7071	0.7071	0
dF 1	(100) (010)	57	143	28	320*	85	0.6322	0.7744	0.0253
dF 1	(100) (−110)	57	143	89	170	32	0.6117	0.7910	0.0081
dF 1	(010) (−110)	28	140	89	170	61	0.6463	0.763	0.088
dF 2	(100) (010)	10	175	30	85	85	0.1073	0.5055	−0.8561
dF3	(100) (010)	10	106	30	4	85	0.4647	0.2869	−0.8357
CF 1	(100) (010)	55	156	30	335*	85	0.4180	0.9084	0.0087
CF1	(100) (−210)	55	156	13	240*	76	0.7666	−0.2899	0.5729
CF1	(010) (−210)	30	155	13	240*	79	0.5132	0.0682	0.8555
CF 2	(100) (010)	10	111	28	10	85	0.4065	0.3178	−0.8566
aF 1	(100) (010)	57	180	28	0	85	0	1	0
aF 2	(100) (010)	16	180	79	0	85	0	1	0
aF 3	(100) (010)	16	140	79	320*	85	0.6428	0.766	0
AB 1 hyp	(100) (010)	55	12	30	192	85	0.2079	0.9781	0
AB 2	(100) (010)	12	150	30	253*	85	0.4183	0.3723	0.8285
AB 3	(100) (010)	12	228	30	305	85	−0.5189	−0.2248	−0.8285
bB1	(100) (010)	57	24	28	205	85	0.4185	−0.9082	−0.0084
CB 1	(100) (010)	55	33	30	214*	85	0.5550	−0.8318	−0.0087
CB 2	(100) (010)	10	70	85	240*	85	0.9387	−0.3145	−0.015
CB 3	(100) (010)	10	352	85	339*	85	−0.1425	−0.9896	−0.0194
dB1	(100) (010)	55	40	30	222*	85	0.6615	−0.7497	0.0174

[a] The number indicates the type of orientation populations: (1) principal high intensity reflection (appears in black on Fig. 2 and 4); (2, 3) other families with lower intensities (appear in gray on Fig. 2 and 4). AB1 hyp, hypothesis, which comes from the calculation of the middle of AB pole figure that is not present because of missing experimental data; *, +180°, that is, to have correct values between two planes 180° have been added to some ψ_2 angles.

plicated, less accurate, and difficult to interpret for all the samples. Table III gives an example of calculation showing the complete disagreement [CF1 with (−210)] between (100) and (010) with (−210), which are not coherent concerning dihedral plane angles.

The figure for the AB (100) pole is less accurate, probably because of experimental failure, but appears to follow the trend with the (010) pole and also when compared to the neighbor sample (AB compared to CB). The main pole angle value for (100) and (010)

TABLE IV
Orientation of Chains with Respect to Sample Positions in Machine Direction (MD) or Transverse Direction (TD)[a]

Sample	Latitude of *c* axis (°)	Meridian of *c* /MD	*c* angle /TD	Chain angle /TD
dF1	0.7	51	−39	±5
CF1	0.5	65	−25	±5
AF1	0	90	0	±5
AB1	0.25	−78	12	±5
bB1	−0.5	−65	15	±5
CB1	−0.5	−56	24	±5
dB1	0	−48	32	±5
dF annealed	−0.5	45	−45	±5
dF2	−58	−78	2	*
dF3	−57	32	−58	*
CF2	−57	38	−52	*
AF2	0	90	0	±6
AF3	0	50	−40	±6
AB2	56	42	−48	*
AB3	−56	−24	66	*
CB2	0.85	−20	70	±1
CB3	1.1	82	−8	±1

[a] The number is used to distinguish between orientation populations: 1, principal population, which is the first part of the table; 2 and 3, secondary populations, which are in the last part of the table. *, not in the film plane.

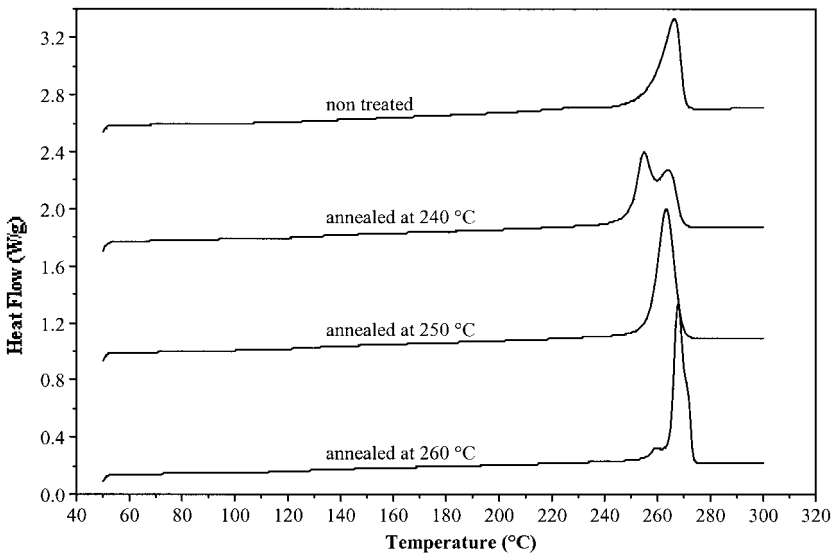

Figure 5 DSC analysis of dF PEN samples.

shown in Table III can then be calculated to be used as a hypothesis for coherence of all the other results (AB1 hyp).

It is worth noting that crystals are completely perpendicular to the machine direction in the center of the film (aF and approximately AB). This is attributed to the transverse stretching made after the longitudinal stretch on the hot foil. This has been observed for other polymers sequentially oriented.[15]

PEN films showed large variation of texture according to the transversal position of the sample, as shown in Table IV. The systematic studies relating the texture with the width position of the sample show that at the edges the texture is tilted by approximately 45° with respect to the machine direction. The tilt is related to the initial stages of transverse drawing when the edges of the ribbon are being gripped and pulled transversally. The shear and drawing, acting with a significantly high rate, stimulate the crystallization of PEN in a tilted manner.

Concerning annealing at 260°C, Figure 4 shows that minor orientations disappear and that the main orientation is modified. This could be attributable to a melting of this secondary phase and recrystallizing without orientation afterward with probably some amorphous phase (see the following two sections). Thus the reflection plane (−110) is situated at the upper pole and the plane of the chain is parallel to the film within ±5°. Dielectric analysis has also allowed the observation of the evolution of molecular relaxation phenomena with morphology changes when disorientation occurs in the amorphous phase[16] and FTIR polarized measurements have quantified the disorientation occurring when annealing takes place.[17]

DSC analysis

The DSC thermograms of four differently thermally treated PEN samples, taken in the dF position (the same as those taken to produce Fig. 4), are shown in Figure 5. The thermal treatment was carried out for 1 h at temperatures of 240, 250, and 260°C. The glass-transition temperature occurs close to 118°C and the melting temperature from 230 to 270°C, as can be seen in Table V. Two values for the 100% crystalline enthalpy can be found in the literature: ΔHf_∞ = 103.4 J/g[18] or ΔHf_∞ = 190 J/g.[19] The crystallinity ratios for the nontreated and the three annealed samples were calculated in this study using ΔHf_∞ = 190 J/g[19] and can be seen in Table V. These values are typical of a semicrystalline bioriented thermoplastic polyester. By use of a custom-developed fitting program, the peaks

TABLE V
DSC Analysis and Peak Decomposition of PEN 25 μm dF Samples[a]

Sample	T_g Onset–Mid (°C)	T_m Peak 1 (°C)	ΔH_1 (J/g)	T_m Peak 2 (°C)	ΔH_2 (J/g)	ΔH Total	Percentage crystallinity
Nontreated	117.5–132.5	233	2.23	267	35.86	38.09	20
Treated 240°C	118.8–133.8	255	22.06	264	22.93	44.99	23.6
Treated 250°C	118.5–133.7	260	8.95	264	37.72	46.67	24.6
Treated 260°C	119.2–136.3	256	4.95	270	43.73	48.73	25.6

[a] T_g, glass-transition temperature; T_m, melting temperature.

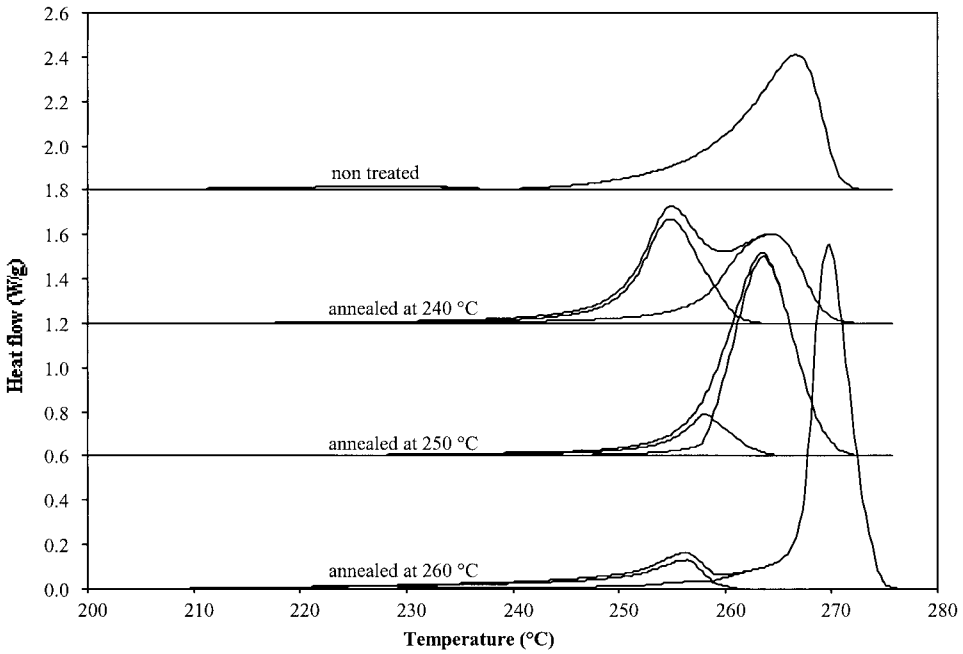

Figure 6 Peak deconvolution of DSC curves.

were decomposed, clearly showing that there are two melting endotherms, as can be seen in Figure 6. Table V gives also the peak positions for the two melting endotherms observed and the respective enthalpies as a function of annealing temperature. The variation of the glass-transition temperature for the four different samples is not significant (±2 K, which is within experimental error range). In contrast, the melting temperatures and crystallinity ratios increase with annealing temperature, which is in agreement with the increase in the size of the crystallites and/or the perfecting of these entities as the annealing temperatures increase. The thermogram of the nontreated sample shows a low melting temperature peak at 233°C, which corresponds probably to the secondary population disappearing on the 240°C annealed sample thermogram. When the annealing temperature increases, the thermograms show two peaks. The first one can be attributed to the recrystallization of the lower peak and also possibly to a partial crystallization of the amorphous phase, some of which is probably oriented. Then, it decreases in intensity and shifts to a higher temperature value. At 260°C it could be assumed that it is completely mixed with that of the oriented phase, whereas the lower temperature peak could be considered as residual unoriented crystals. Concerning the second melting peak, its position remains quite constant and its intensity increases regularly from 240 to 260°C where it has the smaller bandwidth (see Fig. 6). It can be easily seen in Table V that crystallinity increases with annealing temperatures (T_{ann}). For T_{ann} = 250°C, it is more likely expected that the thermogram reflects the temperature of annealing of PEN film in the industrial process (also called thermosetting temperature, which is used to make the film more stable for heat shrinkage).

Thermomechanical analysis

The discussion on the TMA results is totally dependent on the assumption that no TD relaxation has been applied to the film during manufacture.

Thermal shrinkage curves for the three aF, dB, and dF nontreated samples in MD and TD are reported in Figure 7. It can be assumed that it concerns mainly the amorphous phase of the material becoming disoriented from elongated chains, certainly accompanied by crystallization. The highest discrepancy is observed for the aF sample between the MD and TD. The behavior of dF and dB is quite similar in TD and MD, in accordance with a *c*-axis angle close to 45° from the MD (i.e., comparable shrinkage discrepancies). Concerning the center of the film, in the aF position, the amorphous chains oriented in the TD will probably shrink in this direction, which explains the highest transversal shrinkage value observed. Similar results have been obtained for other samples.

CONCLUSIONS

Pole figure measurements have shown a strong dependency on the position in the transverse direction of the film and that there is primarily a dominant crystal population, whose *c*-axis direction varies from +45° at one edge to −45° at the other edge, the orientation at the center being parallel to the transverse direction.

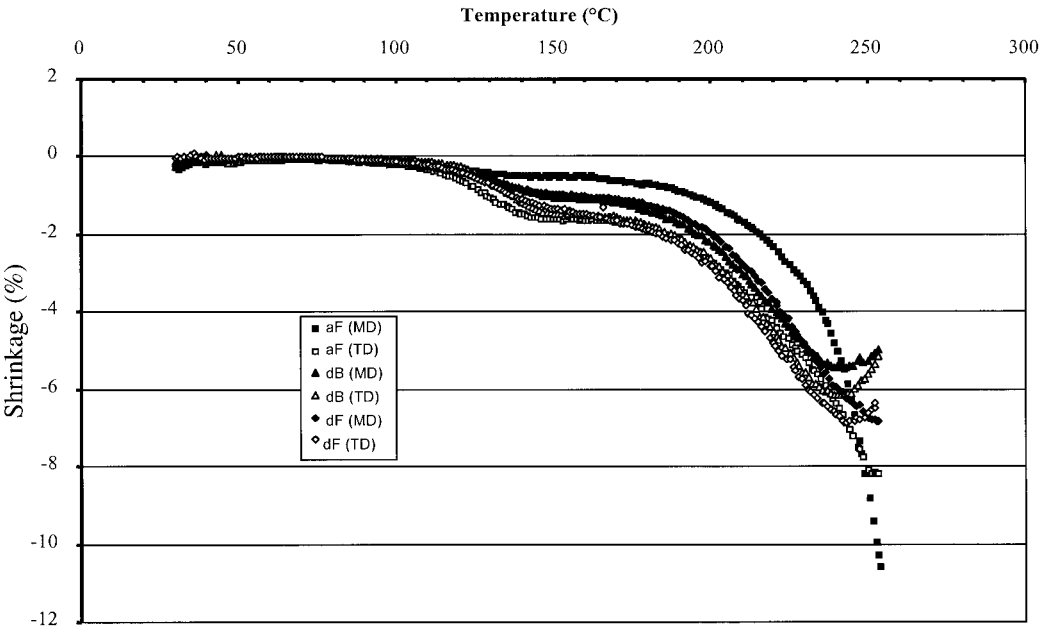

Figure 7 Thermal shrinkage measurements by TMA.

There is also a secondary population, which can be seen only near the center. The transverse orientation in the center is attributed to the two-step drawing of the film, the TD drawing being performed afterward at a temperature above the T_g. It is likely that in a similar way to the crystalline phase, the amorphous phase chains are also highly oriented, as shown by change in the thermal shrinkage evolution measured by TMA, the highest dimensional evolution ratio between TD and MD occurring at the center of the film. DSC measurements strongly confirm these results, given that crystallinity increases with annealing temperature because of a further crystallization accompanied by a disorientation of the oriented amorphous phase demonstrated previously by FTIR.[17] Pole figures have shown that the texture was modified probably attributable to the disorientation mainly from an annealing temperature of 260°C.

According to the literature data, the crystallization of PET[20] is very sensitive to the rate of deformation and less to the degree of deformation. Similar behavior can thus also be assumed to occur for PEN.

The authors thank the Ministry of Education and Research for its support through a Ph.D. grant. Du Pont de Nemours (R. Adam) is thanked for providing the PEN samples. This work was performed within the framework of the bilateral PICS (International Scientific Cooperation Program between Poland and France) exchange program.

References

1. Krause, E. Ph.D. Thesis, Université de Paul Sabatier, Toulouse, France, 1996.
2. Weick, B. L.; Bhushan, B. IEEE Trans Magn 1995, 31, 2937.
3. Weick, B. L.; Bhushan, B. Wear 1995, 190, 28.
4. Mencik, Z. Chem Prümysil 1967, 17, cfs2.
5. Buchner, S.; Wiswe, D.; Zachmann, H. G. Polymer 1989, 30, 480.
6. Cakmak, M.; Wang, Y. D.; Simhambhatla, M. Polym Eng Sci 1990, 30, 721.
7. Murakami, S.; Yamakawa, M.; Tsuji, M.; Kohjiya, S. Polymer 1996, 37, 3945.
8. Murakami, S.; Nishikawa, Y.; Tsuji, M.; Kawaguchi, A.; Kohjiya, S.; Cakmak, M. Polymer 1995, 36, 291.
9. Nakamae, K.; Nishino, T.; Tada, K.; Kanamoto, T.; Ito, M. Polymer 1993, 34, 3322.
10. Nakamae, K.; Nishino, T.; Gotoh, Y. Polymer 1995, 36, 1401.
11. Rueda, D. R.; Viksne, A.; Malers, L.; Balta-calleja, F. Macromol Chem Phys 1994, 195, 3869.
12. Jungnickel, B. J. J Polym Sci Polym Phys Ed 1980, 18, 1811.
13. Jungnickel, B. J. Prog Colloid Polym Sci 1980, 67, 159.
14. Hardy, L.; Stevenson, I.; Boiteux, G.; Seytre, G.; Schönhals, A. Polymer 2001, 42, 5679.
15. Bartczak, Z.; Martucelli, E. Polymer 1997, 38, 4139.
16. Hardy, L.; Fritz, A.; Stevenson, I.; Boiteux, G.; Seytre, G.; Schoenhals, A. J Non-Cryst Solids 2002, 305, 174.
17. Hardy, L.; Stevenson, I.; Voice, A.; Ward, I. M. Polymer 2002, 43, 6013.
18. Cakmak, M.; Lee, S. W. Polymer 1995, 36, 4039.
19. Cakmak, M.; Kim, J. C. J Appl Polym Sci 1997, 64, 729.
20. Zaruli, J. S.; Boyce, M. C. Polymer 1997, 38, 1303.